

Formulation of Single Event Burnout Failure Rate for High Voltage Devices in Satellite Electrical Power System

Yuji Shiba, Erdenebaatar Dashdondog, Masaki Sudo and Ichiro Omura

Electrical Engineering and Electronics

Kyushu Institute of Technology

1-1 Sensui-cho, Tobata-ku, Kitakyushu 804-8550, JAPAN

p349516y@mail.kyutech.jp, omura@ele.kyutech.jp

Abstract—Single-Event Burnout (SEB) is a catastrophic failure in the high voltage devices that is initiated by the passage of particles during turn-off state. Previous papers reported that SEB failure rate increases sharply when applied voltage exceeds a certain threshold voltage. On the other hand, the high voltage devices for the artificial satellite have been increasing. In space, due to increase flux of particle, it is predicted that SEB failure rate will be higher. In this paper, we proposed the failure rate calculation method for high voltage devices based on SEB cross section and flux of particles. This formula can calculate the failure rate at space level and terrestrial level depending on the applied voltage of the high voltage devices.

Keywords—Single Event Burnout; failure rate; cosmic rays; high voltage devices;

I. INTRODUCTION

Single Event Burnout (SEB) is a catastrophic failure in the high voltage devices that is initiated by the passage of particles during turn-off state. Since 1994, SEB failure rate has been reported that it depends exponentially on the applied voltage and nearly independent on temperature [1, 2, 3, 4]. SEB failure is caused by the avalanche phenomenon. The trigger is a charge generated by particles passing through the device. If energy of particle increases, it causes avalanche phenomenon to start at low voltage [5]. The effective method to reduce the failure rate is device design reducing the maximum electric field within the device.

The space industry market and manufacturing have been increased for last decades. It seems that the trend will be kept increasing as well [6]. To reduce the loss of the artificial satellite, along with multi-functionalization, it is expected to increase voltage. Power devices are key component for power conversation in the artificial satellite with increasing multi-functionality, and high breakdown voltage devices are required. For high voltage devices, the tolerant design for cosmic ray induced failure is important. In space, there are more particles than sea level; the failure rate is expected to increase [7]. It is difficult to do experiment for very high energy of particles collision, and the failure rate in space can't be predicted.

In this paper, we proposed that the failure rate calculation method for high voltage devices based on SEB cross section and flux of particles. This method uses formula which can calculates the failure rate of high voltage devices at space level and sea level, depending on the applied voltage on it.

II. PROPOSAL FORMULA OF FAILURE RATE CALCULATION METHOD FOR HIGH VOLTAGE DEVICES

Equation (1) is structure of the proposal failure rate calculation method formula. Proposed failure rate calculation method is based on SEB cross section $\sigma(V_{DC})$ and the flux of particles $Flux(E_p)$. The failure rate FR is expressed by adding the each failure rate of different energy of flux. α is coefficient that convert failure rate dimensions from sec^{-1} to FIT. Equation (2) is structure of SEB cross section $\sigma(V_{DC})$. It is consist of the

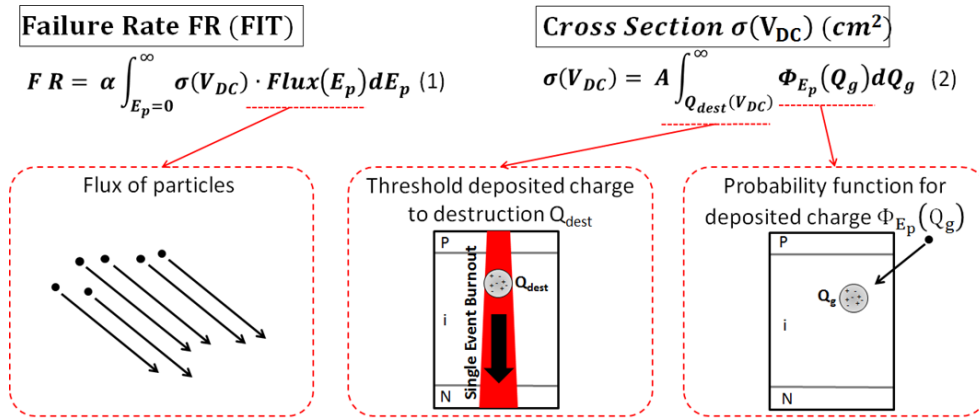


Fig. 1. Structure of failure rate calculation method formula

threshold charge to destruction $Q_{dest}(V_{DC})$ and probability function for generated charge $\Phi_{Ep}(Q_g)$. The cross section means the probability that some charges are generated by one particle. In proposed formula, SEB cross section $\sigma(V_{DC})$ express the probability of the charge generation which can be cause of the device failure at the certain value of applied voltage. So that a low limit of integral range of formula represents threshold charge to destruction $Q_{dest}(V_{DC})$. Also, SEB cross section $\sigma(V_{DC})$ depends on applied voltage. The parameter names and units of symbols used in equation (1) and (2) are listed in Table 1.

Table 1. Parameter names and units of symbols used in equation (1) and (2)

Symbol	Parameter name	unit
FR	Failure rate	FIT
α	Convert from sec to FIT	$3600 \times 10^9 s$
$\sigma(V_{DC})$	Cross section	cm^2
$Flux(E_p)$	Flux of particles	$MeV^{-1}s^{-1}cm^{-2}$
E_p	Particle energy	MeV
A	Device area	cm^2
$\Phi_{Ep}(Q_g)$	Probability function for generated charge	$C^{-1}\mu m^{-1}$
Q_g	Generated charge	C
$Q_{dest}(V_{DC})$	Threshold charge to destruction	C

In order to establish our proposed formula, three parameters were considered. Firstly, threshold charge to destruction $Q_{dest}(V_{DC})$ was analyzed by TCAD simulation with 3.3-kV PiN Diode model. Secondly, probability function for generated charge $\Phi_{Ep}(Q_g)$ were calculated from literatures [8, 9]. Thirdly, we obtained the terrestrial neutron flux data [10] and the space proton flux data from STE-QUEST mission [11] and PAMELA data [12]. By using the above three parameters, the failure rate can be calculated. Detail will be explained in next section.

III. THREE MAIN PARAMETERS DEPENDING ON SINGLE EVENT BURNOUT FAILURE

A. Threshold generated charge to destruction $Q_{dest}(V_{DC})$

SEB failure is caused by the avalanche phenomenon. Particles penetrate into the device and deposit energy, that energy transfer to charge generation which expressed Q_g . SEB failure occurs when the generated charge Q_g exceed to a certain amount of charge, which causes avalanche phenomenon. We named it by threshold charge to destruction $Q_{dest}(V_{DC})$.

We analyzed $Q_{dest}(V_{DC})$ with 3.3-kV PiN diode in TCAD simulation. A cylindrical structure with a 400 μm radius was used. The structure consists of highly doped N-layer and P-layer, and lightly doped 350 μm N-base between these highly doped layers. Position of the energetic particle penetration is the center axis of the cylindrical structure, and it is 10 μm deep from the boundary between P-layer and N-base toward N-base that path includes generated charge Q_g . The radial distribution of the generated charge was determined by a Gaussian distribution with a characteristics length of 0.02 μm .

Figure 2 shows the charge generation as a function of applied voltage for different particle energy. When the

generated charge Q_g becomes larger than certain amount, then avalanche phenomenon starts. The value of generated charge Q_g that triggers avalanche phenomenon starting was determined as the threshold charge to destruction $Q_{dest}(V_{DC})$, which has a function of the applied voltages. We obtained values of threshold charge to destruction $Q_{dest}(V_{DC})$ from three kinds of energy of particle cases (10 MeV, 50 MeV and 100 MeV).

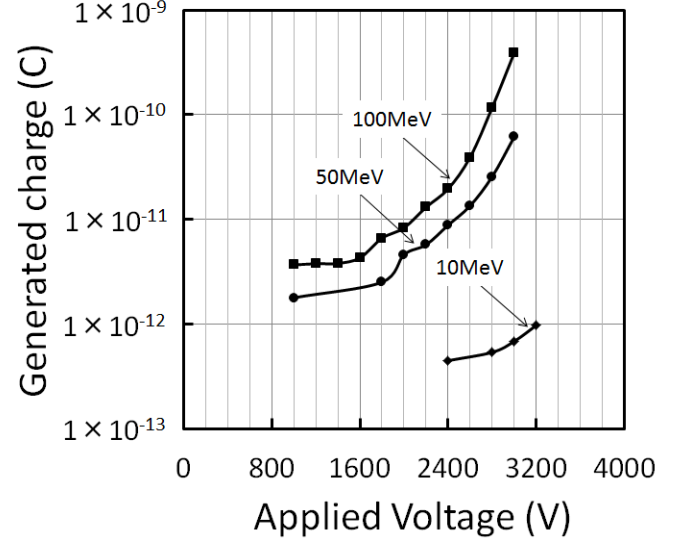


Fig. 2. Generated Charge as a function applied voltage obtained from TCAD simulation for different energy of particle in 3.3-kV PiN diode.

From these results, as shown in Figure 3, approximate curve of threshold charge to destruction $Q_{dest}(V_{DC})$ was drawn as a function of applied voltage. It shows that $Q_{dest}(V_{DC})$ exponentially depends on applied voltage.

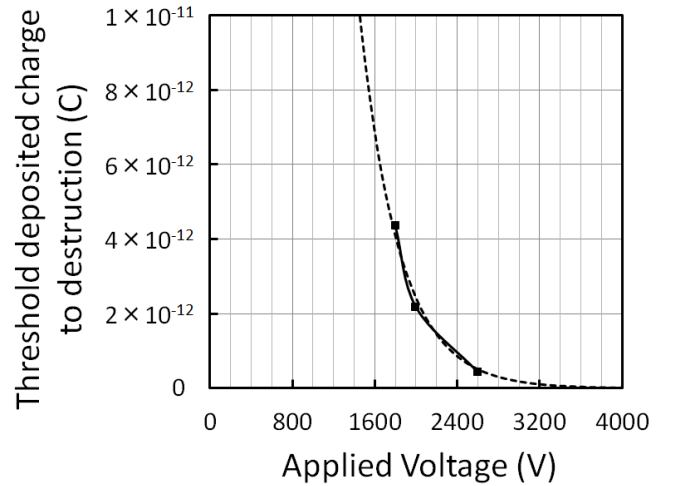


Fig. 3. Relationship between threshold generated charge to destruction Q_{dest} and applied voltage

B. Probability function for deposited charge $\Phi_{Ep}(Q_d)$

Previous papers showed the probability function for deposited energy E_d from some particle energies [8, 9]. Probability function was reported that it is expressed by equation 3 when deposited energy E_d is 2 MeV or more [8]. Basically, we can see that, deposited energy function consists of two parameters decreasing exponential function. There are b_1 and b_2 in equation 3. b_1 is the slop and b_0 is the intercept in the probability function. We obtained probability function for deposited charge $\Phi_{Ep}(Q_d)$ by deciding b_1 and b_0 for particle energies and converting energy into charge.

$$\phi_{E_p}(E_d) = 10^{b_1(E_p) \cdot E_d + b_0(E_p)} \quad (3)$$

In the previous papers, low particle energy condition was analyzed ($E_p \leq 100$ MeV) and we obtained b_1 and b_2 for neutrons (neutron energies are 20, 50 100 MeV) [9]. For higher particle energy, it was described that b_1 and b_0 are saturated. We approximated the saturation values by fitting three points.

We assumed that, deposited energy by particle penetrating into the device completely generated electron-hole pairs. In other words, generated charge Q_g is linearly depends on deposited energy E_d . In silicon case, the band gap energy E_g required to create an electron-hole pair is $E_g \approx 3.68$ eV. The pair charge is $q = 1.6 \times 10^{19}$ C. Hence, coefficient $\beta = 0.43 \times 10^{-13}$ C/MeV, which shows relation between deposited charge Q_d and deposited energy E_d has been found ($Q_d = \beta \cdot E_d$).

Figure 4 shows Probability function for deposited charge $\Phi_{Ep}(Q_g)$ for 10^6 particles. The probability function for generated charge $\Phi_{Ep}(Q_g)$ is showed for the particle energy from 30 MeV to 100 MeV. From 30 MeV to 300 MeV, the gradient of the probability function for generated charge $\Phi_{Ep}(Q_d)$ becomes gentle as the particle energy increases. Probability function for generated charge $\Phi_{Ep}(Q_d)$ of 50 MeV and 100 MeV are almost same as corresponding experimental results reported in [9]. Probability function for g charge $\Phi_{Ep}(Q_d)$ is almost constant when incident energy of the particle is over 300 MeV. For high particle energy, it shows that SEB cross section is saturated. This result is also similar to corresponding result reported in [8].

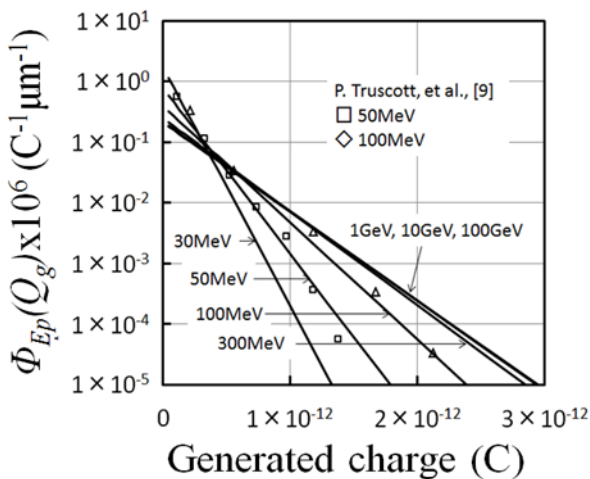


Fig. 4. Probability function for deposited charge $\Phi_{Ep}(Q_d)$ for 10^6 particles.

C. Flux of particles $Flux(E_p)$

In space, 90 % of those particles consist of protons [14]. Since the Earth is protected by geomagnetism, the proton, which is an electric particle, is bent or confined in the geomagnetism. Among them, the protons that fall down to the Earth collide with molecules in atmosphere of the Earth and it makes neutron shower. Therefore, we calculated the failure rate with terrestrial neutron flux at sea level and space proton flux in space.

Figure 5 shows the terrestrial neutron flux and space proton flux. The terrestrial neutron flux data is analytic model by M. S. Gordon, et al. [10]. Space proton flux data have two kinds of data, which is difference altitude and proton energy. One is a STE-QUEST mission data [11] and the other is PAMELA data [12]. We approximated function of the two space proton flux data. At about 1 MeV - 500 MeV space proton flux data, which measured at around altitude of 800 km - 2400 km and its fitted function were taken from STE-QUEST mission data source. Also, we obtained aluminum shielding space proton flux data at same condition, too. At 1 GeV - 150 GeV space proton flux data, which measured at around 350 km - 610 km and its fitted function were taken from PAMELA data source.

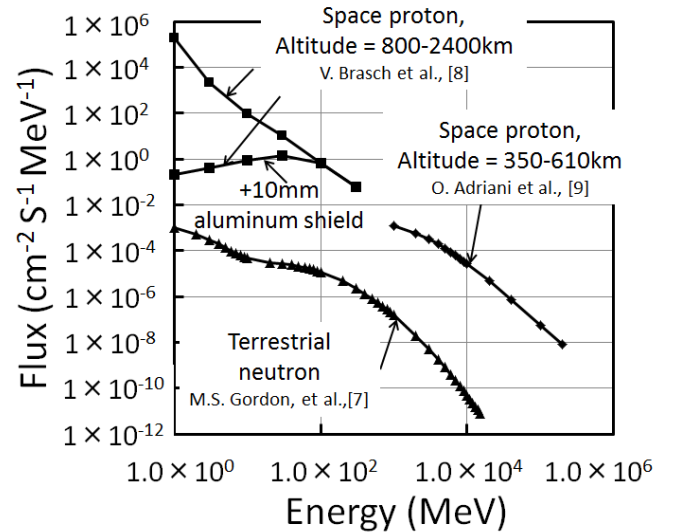


Fig. 5. The terrestrial neutron flux and the space proton flux. Also, aluminum shield effect to proton flux data.

IV. FAILURE RATE CALCULATION FOR 3.3-kV PiN DIODE

The failure rate of 3.3-kV PiN Diode was calculated by our proposed calculation method at sea level and in space. In space, the failure rate can be expressed as one function, even with multiple flux of particles $Flux(E_p)$. The reason is that the failure rate is the sum of the failure rates for the each particle energy. The failure rate depends strongly on flux of particles $Flux(E_p)$ and threshold charge to destruction $Q_{dest}(V_{DC})$. Figure 6 shows that up to $V_{DC} = 2200$ V, the failure rate difference between at sea level and in space is flux. In this voltage range, the failure rate increase as satellite orbit gets higher. Below about $V_{DC} = 2200$ V, the failure rate drops suddenly, it is influenced by threshold charge to destruction $Q_{dest}(V_{DC})$. Threshold charge to destruction $Q_{dest}(V_{DC})$ increases

exponentially if applied voltage is decreased beyond that point. Therefore, the failure rate is decreased at low applied voltage. From these result, it is possible to ensure the reliability of high voltage devices in satellite electrical power system. Also, we confirmed that there is no effect of aluminum shield because high energy proton does not prevent to penetrate into devices.

In our result, since generated charge Q_g position is the most electric field, the failure rate is considered to be high. In experience, charge generations positions were in various points.

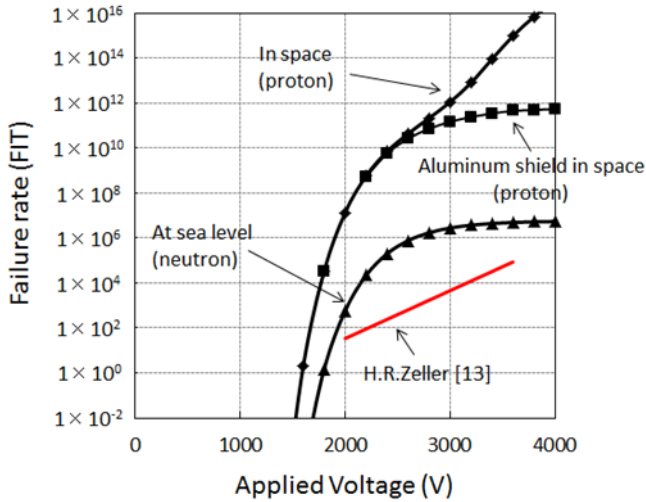


Fig. 6. The failure rate of 3.3-kV PiN diode calculated by our proposed calculation method at the sea level and at satellite orbit level.

V. CONCLUSION

We proposed the failure rate calculation method for high voltage devices based on SEB cross section and flux of particles. In order to establish our proposed formula, three parameters were considered. Firstly, threshold charge to destruction $Q_{dest}(V_{DC})$ was analyzed by TCAD simulation with 3.3-kV PiN Diode model. Secondly, probability function for generated charge $\Phi_{Ep}(Q_g)$ were calculated from literatures [8, 9]. Thirdly, we obtained the terrestrial neutron flux data [10] and the space proton flux data from STE-QUEST mission [11] and PAMELA data [12]. From the result we can see that failure rate in space is apparently higher than at sea level (assumed FIT= 1).

REFERENCES

- [1] H. Kabza, H. J. Schulze, Y. Gerstenmaier, P. Voss, J. W. W. Schmid, F. Pfirsch and K. Platzoder, "Cosmic radiation as a cause for power device failure and possible countermeasures," Proc. of ISPSD'94, pp. 9-12, 1994.
- [2] H. R. Zeller, "Cosmic ray induced breakdown in high voltage semiconductor devices, microscopic model and phenomenological lifetime prediction," Proc. of ISPSD'94, pp. 339-340, 1994.
- [3] A. M. Albadri, R. D. Schrimpf, D. G. Walker and S. V. Mahajan, "Coupled electro-thermal Simulations of single event burnout in power diodes," IEEE Trans. on Nucl. Sci., Vol. 52, No. 6, pp. 2194-2199, 2005.
- [4] C. Felgemacher, S. V. Araújo, P. Zacharias, Karl Nesemann, A. Gruber, "Cosmic radiation ruggedness of Si and SiC power semiconductors," Proc. of ISPSD'16, pp. 52-55, 2016.

- [5] G. Soelkner, W. Kaindl, H. J. Schulze, G. Wachutka, "Reliability of power electronic devices against cosmic radiation-induced failure," Microelectron. Reliab. Vol 44, No. 9 pp. 1399-1406, 2004.
- [6] J. R. Brophy, R. Gershman, N. Strange and D. Landau, "300-kW solar electric propulsion system configuration for human exploration of near-earth asteroids," 47th AIAA/ASME/SAE/ASEE Joint Propulsion Conference & Exhibit, AIAA 2011, pp. 2011-5514.
- [7] A. M. Albadri, R. D. Schrimpf, K. F. Galloway and D. G. Walker, "Single event burnout in power diodes: Mechanisms and models," Microelectron. Reliab., Vol. 46, No. 2-4, pp. 317-325, 2006.
- [8] B. Doucin, Y. Patin and J. P. Lochard, "Characterization of proton interactions in electronic components," IEEE Trans. Nucl. Sci., Vol. 41, No. 3, pp. 593-600, 1994.
- [9] P. Truscott, C. Dyer, A. Frydland, A. Hands, S. Clucas and K. Hunter, "Neutron Energy-Deposition Spectra Measurements, and Comparisons with Geant4 Predictions," Proc. of RADECS'05, pp. LN11-1-LN11-4, 2005.
- [10] M. S. Gordon, P. Goldhagen, K. P. Rodbell, T. H. Zabel, H. H. K. Tang, J. M. Clem and P. Bailey, "Measurement of the flux and energy spectrum of cosmic-ray induced neutrons on the ground," IEEE Trans. Nucl. Sci., Vol. 51, No. 6, pp. 3427-3434, 2004.
- [11] V. Brasch, Q. F. Chen, S. Schiller and T. J. Kippenberg, "Radiation hardness of high-Q silicon nitride microresonators for space compatible integrated optics," Optics Express, Vol. 22, No. 25, pp. 30786-30794, 2014.
- [12] O. Adriani, et al., "PAMELA Measurements of Cosmic-Ray Proton and Helium Spectra," Science, Vol. 332, No. 6025, pp. 69-72, 2011.
- [13] H. R. Zeller, "Cosmic ray induced failures in high power semiconductor devices," Microelectron. Reliab., Vol. 37, No. 10-11, pp. 1711-1718, 1997.
- [14] J.F. Ziegler, "Terrestrial cosmic rays," IBM Journal of Research and Development, Vol. 40, No. 1, pp. 19-39, 1996.